Postharvest Biology and Technology 149 (2019) 27–41

Contents lists available at ScienceDirect

Postharvest Biology and Technology

journal homepage: www.elsevier.com/locate/postharvbio

Co-expression networks provide insights into molecular mechanisms of postharvest temperature modulation of apple fruit to reduce superficial scald

Loren A. Honaas[a,*], Heidi L. Hargarten[a], Stephen P. Ficklin[b], John A. Hadish[b], Eric Wafula[c], Claude W. dePamphilis[c], James P. Mattheis[a], David R. Rudell[a]

[a] USDA, ARS, Tree Fruit Research Laboratory, Wenatchee, WA, 98801, USA
[b] Department of Horticulture, Washington State University, Pullman, WA, 99164, USA
[c] The Huck Institutes of the Life Science and The Biology Department, Penn State, University Park, PA 16802, USA

ARTICLE INFO

Keywords:
Transcriptome
Co-expression network
RNA-Seq
'Granny Smith'
qPCR

ABSTRACT

Temperature conditioning is an effective approach for enhancing some aspects of postharvest apple fruit quality, particularly avoidance of chilling injury. The molecular mechanisms of warming regimes that alter apple fruit quality are poorly understood, as is how warming contributes to avoiding development of the peel disorder superficial scald. Here we report transcriptional responses of 'Granny Smith' fruit peel during the early phases of long-term cold storage in response to intermittent warming, an ostensibly organic compliant strategy that effectively reduced scald incidence. We observed two temporally distinct classes of gene expression, which were discovered by co-expression network analyses. One profile is largely concordant with recovery from chilling stress, whereas the other reveals transient shifts marked by hormone signaling and transcription and translation machinery. Altogether, our analyses point to novel aspects of superficial scald etiology and circumscribes a list of candidate genes that may be useful to uncover molecular processes that promote, as well as mitigate, the peel disorder.

1. Introduction

Superficial scald is a disorder of apple (*Malus* × *domestica* Borkh.) fruit epidermal tissues, characterized by darkened necrotic lesions (Lurie and Watkins, 2012). The relationship between storage conditions and superficial scald severity typify a chilling-related disorder (Watkins et al., 1995), though the extended period of time between chilling stress and appearance of symptoms (on the order of months in extended storage) reveal temporally distinct events during disorder progression (Bramlage and Meir, 1990). Previous work has suggested that oxidative stress (Watkins et al., 1995), provoked by putative oxidation products of α-farnesene (Gapper et al., 2017; Rowan et al., 2001), leads to apple fruit peel necrosis.

In 'Granny Smith' and other susceptible apple cultivars this disorder is well controlled with conventional crop protectants like diphenylamine (DPA) and 1-methylcyclopropene (1-MCP) (Gapper et al., 2017). The former is a potent antioxidant that inhibits α-farnesene oxidation (Huelin and Coggiola, 1970) the latter a highly effective competitive inhibitor of ethylene action (Mattheis et al., 2017; Mattheis, 2008; Sisler et al., 2003). Other methods of disorder mitigation include controlled atmosphere (CA) storage, dynamic CA regulated by chlorophyll fluorescence, oil wraps, and temperature conditioning – especially intermittent warming early in the cold storage period (Lurie and Watkins, 2012). Recent work has been focused on superficial scald control using DPA and/or 1-MCP (Busatto et al., 2018; Gapper et al., 2017; Zermiani et al., 2015). However, relatively little is known of the molecular mechanisms of control using crop protectant-limited postharvest practices, like intermittent warming, which can be as effective as conventional practices. This is especially relevant in an apple fruit marketplace where the proportion of crop protectant-limited fruit production is increasing (Granatstein et al., 2016).

Insights into the molecular mechanisms of temperature conditioning in apple fruit is relevant not only to superficial scald in 'Granny Smith' apple fruit, but also its use to mitigate disorders of the high-value 'Honeycrisp' cultivar (soft scald, soggy breakdown) (Watkins et al., 2004). Here, we focus on superficial scald in 'Granny Smith' apple fruit because of its relevance to the apple fruit industry, but also because it can serve as a model postharvest storage disorder. Superficial scald,

* Corresponding author at: Physiology and Pathology of Tree Fruits Research, USDA-ARS, 1104 N. Western Ave., Wenatchee, WA, 98801, USA.
E-mail address: loren.honaas@ars.usda.gov (L.A. Honaas).

https://doi.org/10.1016/j.postharvbio.2018.09.016
Received 19 June 2018; Received in revised form 22 September 2018; Accepted 22 September 2018
Available online 27 November 2018
0925-5214/

unlike some other disorders, is effectively managed by a host of relevant postharvest practices and is straightforward to induce, allowing reliable contrasts in the annually cropped apple fruit system. The tractability of this disorder makes it potentially useful for the development of novel postharvest technology. This includes tools for diagnostics and risk assessment that target the molecular genetic basis of these complex plant traits.

Here we describe experiments in 'Granny Smith' apple fruit that shed light on molecular mechanisms of superficial scald mitigation by the proven practice of intermittent warming during cold storage in air. Importantly, we developed contrasts of symptom development without the use of potent antioxidant or a highly effective suppressant of ethylene signaling, offering insights into the physiology of the disorder that are free of chemical perturbations. To explore the molecular mechanisms that underpin the intermittent warming response, we used a forward genetics approach. We combined a differential gene expression analysis to identify genes that responded strongly to experimental treatments with a gene co-expression network analysis that identified clusters of genes that responded in a coordinated fashion to experimental treatments. We then examined the functional profiles of these gene collections and developed hypotheses about the molecular mechanisms of superficial scald prevention by intermittent warming.

2. Materials and methods

2.1. Experimental design

'Granny Smith' apples were obtained the day of harvest, 13 September, 2016, from a commercial orchard near Wenatchee, WA, USA. The fruit was hand sorted onto pressed fiber trays and trays were subsequently placed into cardboard boxes. Boxed fruit was then stored at 1 °C in air. All tissue samples were collected in the mid-afternoon. See Table 1 and Supplemental Fig. 1 for sample information.

Fruit peel was collected at harvest and after storage from three replicates of six apples each using a vegetable peeler. Evenly spaced peel sections (n = 3 for each fruit, ~20 cm × 2 cm) cut from the stem end to calyx end, and centered at the equator, were immediately flash frozen in liquid nitrogen and stored at −80 °C. For each sample, one tray of 18 fruit was used for RNA collection, while three additional trays (n = 54 fruit) were stored at 1 °C for visual rating of superficial scald at four, five, & six months, and then rating and destructive quality measurements at six months plus seven days at 20 °C in a simulated supply chain period.

2.2. Diphenylamine (DPA) treatment

DPA was prepared fresh for each treatment by dissolving, with sonication, 8 g DPA in 24 mL of a 1:2 isopropanol:Triton x-100 solution. An emulsion was prepared at 2 g/L DPA (24 mL of the above DPA solution into 4 L water) and was applied to fruit in a bath in which fruit were submerged for ~1 min, then placed on drying trays for at least 1 h in ~1–3 °C. Fruit were then replaced onto original trays before being boxed and returned to cold storage.

2.3. Superficial scald ratings and quality assessment

Superficial scald symptoms were assessed at four, five, and six months after harvest. Fruit were removed from cold storage briefly to rate symptom severity. Scald severity was determined based on the amount of peel surface area affected, rated on a scale from 1 to 5: 1 = no scald, 2 = 1–25 %, 3 = 2 6–50 %, 4 = 51–75 %, 5 = 76–100 % of peel with visible scald symptoms. At 6 months after harvest all apples were removed from cold storage, rated for scald severity, and placed in a dark room at 20 °C for one week to simulate time in the supply chain. After one week, fruit were rated again for scald symptoms and one tray was subject to standard quality measurements as described in Mattheis et al. (2017).

2.4. RNA extraction, quality control, and transcriptome sequencing

Pooled peel tissue was ground to a fine powder in a mortar and pestle in the presence of liquid nitrogen. RNA was extracted using a CTAB/Chloroform protocol modified for use on pome fruit tissue in the postharvest period (Honaas and Kahn, 2017). Extracted RNA was analyzed for quantity and purity using the Nanodrop (Thermo Fisher Scientific, Waltham, MA USA) and for quantity and integrity on the Agilent Bioanalzyer (Agilent, Santa Clara, CA USA, Agilent-RNA Pico Kit, cat#: 5067-1513). Only RNA that met the following standards was used for downstream analysis: A260/A280 ≈ 2.0, RNA Integrity Number (RIN) ≥ 8.0. Libraries were constructed with 600 ng of total RNA at The Penn State Genomics Core Facility in University Park, PA using Illumina's TruSeq Stranded mRNA Library Prep kit (www.illumina.com - RS-122-2103, Illumina San Diego, CA USA) according to the manufacturer's instructions. Libraries were sequenced on a 150 bp single-end protocol to a target volume of ≥20 million reads per biological replicate on Illumina's HiSeq 2500 in Rapid Mode. Read data are publicly available at the Sequencing Read Archive (www.ncbi.nlm.nih.gov/sra – accession number SRP150622).

2.5. Reference selection, processing of transcriptome data, and read mapping

The genome of the commercially produced 'Golden Delicious' cultivar *Mdomestica*_1.0 (Velasco et al., 2010) was selected for use as a reference because: **1)** as of the writing of this manuscript the genome of a double haploid 'Golden Delicious' (GDDH13 Version 1.1 (Daccord et al., 2017)) was not completely annotated and is still being updated to correct errors (see https://iris.angers.inra.fr/gddh13/), **2)** the gene predictions were not reconciled between the two genomes, therefore use of GDDH13 Version 1.0 would require extensive re-annotation and validation – work that is outside the scope of this manuscript, and **3)** our previous analysis Hargarten et al. (2018) showed no improvement in correlation with quantitative real time polymerase chain reaction (qPCR) results for select genes using the GDDH13 v1.1 over the Mdomestica_1.0. Therefore, given these considerations, we decided to use the genome of the commercially produced cultivar, Mdomestica_1.0. The whole genome sequence plus annotation file (*Mdomestica_196_v1.0.fa* with *Mdomestica_196_v1.0.gene.gff3)* and the mRNA predictions (Mdomestica_196_v1.0.tran*script_primaryTranscriptOnly.fa*)

Table 1
Summary of samples for this study.

Sample ID	Description
TC-0	At harvest prior to storage at 1 °C
TC-1, TC-2, TC-3, TC-4	1, 2, 4, & 8 weeks at 1 °C respectively (control)
TE-1, TE-2, TE-3, TE-4	1, 2, 4, & 8 weeks at 1 °C respectively, then 5 days at 20 °C for each time point
T1.1-T1.5	1 week at 1 °C, then 24 h intervals at 20 °C for 5 days (T1.5 is equivalent to TE-1)
RP-2, RP-3, RP-4	Fruit at 20 °C as TE-1, then 20 °C was repeated 2,3, or 4 times at 2,4, & 8 weeks
DT-0, DT-1, DT-2, DT-3, DT-4	Fruit treated with DPA at harvest, then at 1,2,4, & 8 weeks

were retrieved from Phytozome (phytozome.jgi.doe.gov). In pilot read mapping experiments, gene expression estimates using the mRNAs as a reference compared to the whole genome showed better agreement with our qPCR data, therefore the mRNA predictions were selected for the full analysis.

Single-end 150 bp Illumina was first examined with FASTQC (https://www.bioinformatics.babraham.ac.uk/projects/fastqc) to determine the quality of reads and identify embedded and partial TruSeq3 adaptor sequences. Reads were then trimmed to remove adaptor sequences and low-quality regions using Trimmomatic (v0.36) (Bolger et al., 2014) in both simple and palindromic mode. Resulting trimmed reads shorter than 50 bp were discarded. 99.7 ± 0.06% of reads remained after trimming and filtering for a grand total of 558,575,248 reads. Cleaned reads were mapped to the predicted transcripts of Mdomestica_1.0 ((Velasco et al., 2010); *Mdomestica_196_v1.0.transcript_primaryTranscriptOnly.fa*) obtained from Phytozome and expression abundance estimated in a strand-specific mode using the RSEM (v1.3.0) pipeline (Li and Dewey, 2011) with the inbuilt Bowtie2 (Langmead and Salzberg, 2012) read aligner option.

2.6. Validation of RNA-Seq data

RNA-Seq estimates of gene activity were validated on a subset of genes via qPCR. These genes of interest for validation (vGOI, n = 15, Supplemental Table 1) were a subset selected from previous work on superficial scald based on gene activity that was correlated with disorder incidence in that study (Gapper et al., 2017). Susequently, qPCR assays were developed and run for each vGOI as reported in Hargarten et al. (2018). For each vGOI in samples TC-0, TC-1, TC-2, and TE-1 normalized qPCR expression was regressed with normalized RNA-Seq counts (reads per kilobase transcript per million reads – RPKMs). Additionally, vGOI qPCR expression data in all samples for this study was used to help inform sample selection for RNA-Seq analysis in this study (see Supplemental Fig. 1).

2.7. Differential expression (DE) analysis

Estimated gene counts were used for pairwise deferential gene expression and time-course analyses. Pairwise differential gene expression analysis between experimental samples TC-2 and TE-1 was performed with 'DESeq2' (Love et al., 2014) after assembling of estimated count and offset matrices using the R package 'tximport' (Soneson et al., 2015) and filtering out features with only a single count across all samples. Gene clustering was also performed on relative log-transformed values of the filtered expression matrix to determine the amount by which each gene deviates in a sample from the gene's average across all samples. For time-course expression analysis (T1.1-T1.5), the estimated gene count matrices shown in Supplemental File 1 were used to detect genes that show significant expression changes over time using the 'maSigPro' Bioconductor R package (Conesa and Nueda, 2017) with a false discovery rate (FDR) < 0.01, R-squared > 0.7 and clustered using k-means (nine clusters). Expression matrices were normalized using TMM (weighted trimmed mean of M-values) and differential expression analysis performed on genes with CPM (count-per-million) > 1 in at least three samples.

2.8. Network construction

The gene co-expression network was constructed using counts from all sequenced samples (TC-0, TC-1, TC-2, TE-1, and TE1.1-T1.5; See Table 1). Prior to network construction, RPKM values were log2 transformed and RPKM values of 0 were converted to 'NA' indicating a missing value. Next, an outlier test was executed by comparing each sample's expression distribution versus a global distribution of expression across all 27 samples using the Kolmogorov-Smirnov test from the ks.test function in the R base statistical package. No outlier samples were detected. Following outlier detection, log2 transformed expression values were combined into a Gene Expression Matrix (GEM) where samples are the columns and rows are genes from the *Malus x domestica* genome v1.0 (Velasco et al., 2010) available from the Genome Database for Rosaceae (Jung et al., 2014). The cells of the matrix constitute the log2 transformed expression values.

An *n* x *n* similarity matrix was constructed using the Knowledge Independent Network Construction (KINC) package (formerly RMTGeneNet) (Gibson et al., 2013) where *n* is the number of genes. This package has been updated to include identification of sample clusters at the pairwise level using Gaussian Mixture Models (GMM) (Ficklin et al., 2017), with the hypothesis that distinct clusters represent condition-specific gene expression. Therefore, the cells of the similarity matrix are an array of Spearman's rho correlation values—one correlation value for each cluster identified between the pair of genes. KINC uses the MixModLib (Biernacki et al., 2006) package for selection of GMM clusters. KINC was executed on WSU's high-performance computing cluster, Kamiak, using the Integrated Completed Likelihood (ICL) criterion for GMM selection and a limit of 20 observations to accept a cluster for correlation analysis.

Once gene pairwise clusters were identified, and correlation was performed, the 'KINC.R' R package (Ficklin and Shealy, 2016), a helper package for processing KINC output, was used to identify significant edges for the network. To reduce the size of the input file imported to 'KINC.R', a preliminary threshold value of 0.8 was selected and clusters with a Spearman rho value greater than 0.8 were imported into 'KINC.R'. Next, linear regression was performed on all clusters to identify those that were also correlated with warming time. For this, only samples that experienced 24, 48, 72, 96, and 120 h of warming were included in the regression analysis. This was to specifically identify clusters whose expression is a product of warming. Clusters with a linear regression p-value less than or equal to 1 e-7 were then kept and formed a new similarity matrix. To create the final network, Random Matrix Theory (RMT) (Luo et al., 2007) was used to identify a threshold at which the Nearest Neighbor Spacing Distribution (NNSD) of the eigenvalues of the similarity matrix cease to appear Poisson. The threshold identified was ± 0.918 and the final network file was output to a text file suitable for visualization with Cytoscape (Shannon et al., 2003) and includes the regression p-value for warming and a rate of change of the conditional mean for each edge.

After network construction, highly connected subgraphs within the network were identified using the 'linkcomm' (Kalinka and Tomancak, 2011) package of R. The 'linkcomm' package was chosen among other module discovery tools because it allows a node (i.e. a gene) to be in multiple modules. However, the 'linkcomm' package expects that there are no disconnected subgraphs in the network. Therefore, the **findLinkedCommunities** function of the 'KINC.R' package was used to execute the **linkcomm** function for each of the disconnected subgraphs of the network independently. Inverse correlations were removed from the network prior to module discovery to prevent modules from spanning sections of the network that are differentially expressed.

2.9. Heatmap visualization

Clusters in heatmaps correspond to collections of genes (previously defined module genes of interest – m.*x*.GOIs, Supplemental File 2), with no additional clustering of genes applied. For each condition, mean of log2 expression data across all three replicates was calculated and used. Centering of each gene's expression value was done by subtracting the mean log2 expression level from the corresponding condition's log2 expression value. Scaling was then done by dividing this centered expression value by the standard deviation of the feature's (row) expression value (Zhao et al., 2014). These numbers were then mapped to a color scheme where red represents higher expression and blue represents lower expression.

2.10. Functional enrichment analysis of gene of interest (GOIs)

GO function enrichment analysis of GOIs was conducted using the R package 'topGO' (https://bioconductor.org). 'Golden Delicious' apple gene annotations with corresponding GO terms and the best matching *Arabidopsis thaliana* gene were downloaded from Phytozome (Mdomestica_196_v1.0.annotation_info.txt). To generate lists of enriched GO terms, we supplied the **topGOdata** object builder function with a list of the *Malus* gene names and their corresponding GO terms via the **annFUN.gene2GO** function. Using the **topGOdata** object, GO enrichment significance was determined using the **getSigGroups** function with the *"classicCount"* enrichment and *"weight01Count"* algorithm (taking GO hierarchy into account) to execute Fisher's Exact tests for significance. Significant enrichment of GO Terms for each GOI set was calculated for Biological Process (BP) and Molecular Function (MF) ontologies.

3. Results

3.1. Superficial scald incidence and fruit quality

Scald incidence and severity was reduced by all treatments relative to control fruit ($P \leq 5.7$ e-5) (Fig. 1).

Intermittently warmed fruit (TE-1) showed similar scald rates to fruit treated with DPA at the same time (DT-1, $P = 0.87$) (Fig. 2).

Delay of intermittent warming (samples TE-2 through TE-4) and of DPA treatment (samples DT-2 through DT-4) resulted in higher rates of superficial scald and more severe symptoms. DPA treatment just prior to cold storage was most effective at reducing scald, but not by a large margin (One-Way ANOVA, Tukey correction $P = 0.019$) compared to DPA treatment after 1 week. Interestingly, the window of opportunity to mitigate superficial scald with intermittent warming was slightly larger than that for DPA in this experiment (Fig. 1).

Because the storage environment was designed to elicit the disorder, fruit was below market quality in all experimental groups, indicated by low firmness values (Supplemental Fig. 2), and low integrated overall quality (Supplemental Fig. 3). Ethylene concentration was very high (e.g. average 500–1400 ng μL-1) and varied widely both within and among experimental groups, with most experimental groups having significantly higher ethylene concentrations than control fruit (Supplemental Fig. 4). Generally, fruit that had experienced any time at 20 °C had higher ethylene and lower firmness. A minor storage anomaly caused the storage temperature to drift slightly up by ~3 °C over the course of several days between four (~T3) and eight (~T4) weeks of storage. This is not expected to impact the results as all fruit were stored in the same room and experienced the same event which did not coincide with any warming treatments. This suggests warming regimes are as robust to this type of anomaly as the use of DPA.

3.2. Selection of samples for transcriptome sequencing

Our sampling strategy was to generate more samples that we intended to sequence, then use the horticulture data combined with targeted gene expression analysis of the (previously selected) vGOIs to

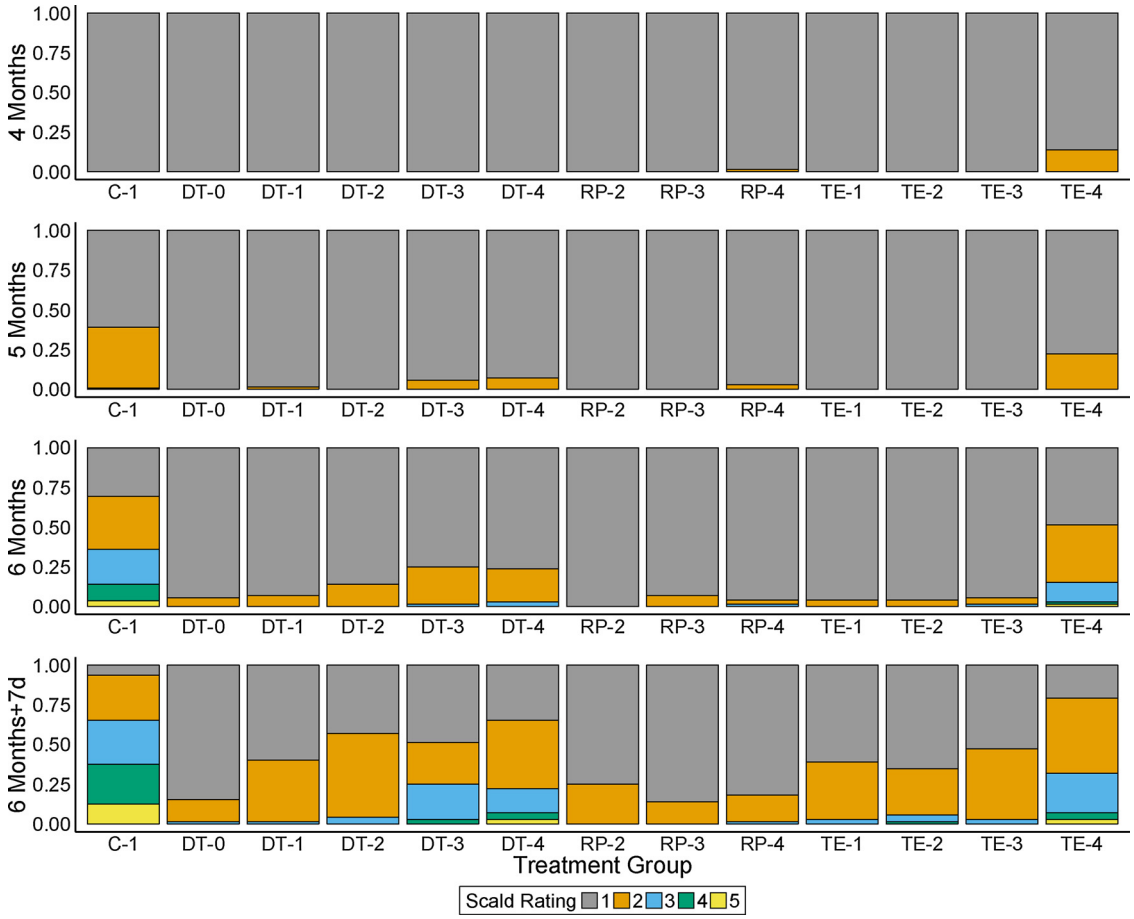

Fig. 1. Control fruit show significantly more scald, and more severe scald, than other experimental treatments. Stacked bar chart showing prevalence and severity of scald at each rating time point (four, five, six months, and six months plus supply chain simulation – 7 d at 20 °C). Scald rating of 1 = no symptoms, 2 = 0–25 % symptomatic peel, 3 = 25–50 % symptomatic peel, 4 = 50–75 % symptomatic peel, 5 = 75–100 % symptomatic peel. All experimental treatments showed significantly less disorder incidence compared to controls (ANOVA, $P < 5.7$ e-5).

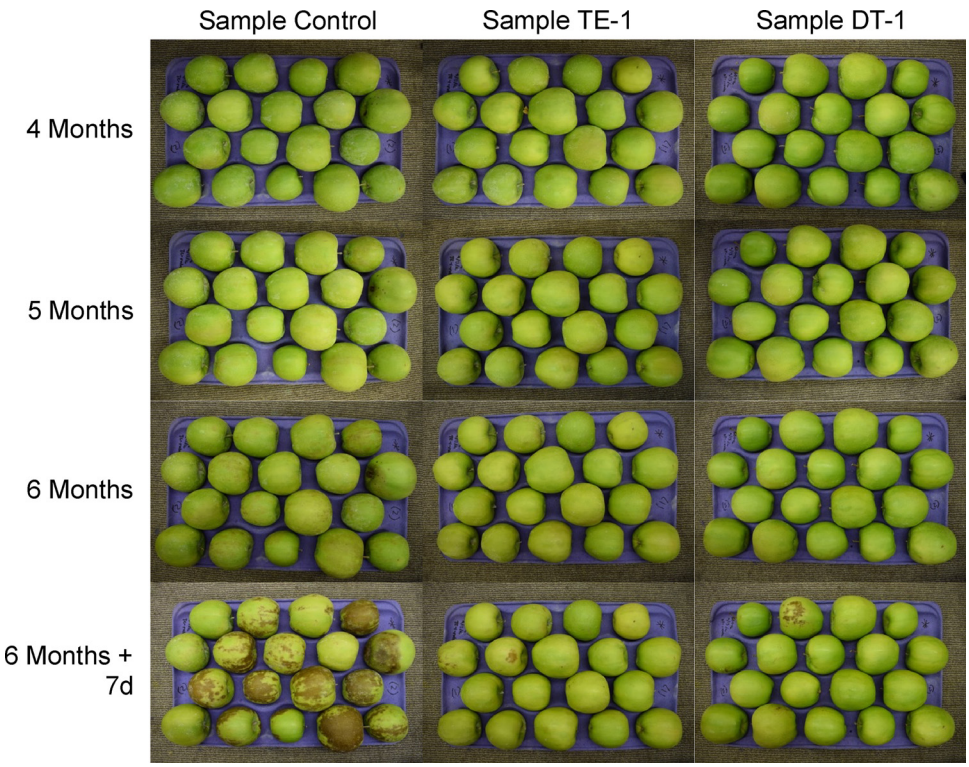

Fig. 2. Intermittent warming was as effective as the antioxidant DPA to reduce superficial scald. Representative sample of the progression of scald incidence across select treatments after four, five, six months of cold storage, plus 7 d of simulated supply chain removal after six months of cold storage. Intermittent warming was 20 °C for 5 d (TE-1), DPA was applied to fruit at the same time warmed fruit was pulled and placed in 20 °C (DT-1). Both treatments had significantly less scald incidence after storage compared to control fruit ($p < 0.001$).

select the best samples for transcriptome analysis. This approach would verify the reproduction of previously reported horticulture results (Watkins et al., 1995) and show us where to focus our global-scale gene expression analysis. The horticulture data indicated that comparison of the control fruit during the first two weeks of cold storage (TC-0, TC-1, and TC-2) with the first intermittently warmed fruit (TE-1) would likely reveal genes of interest.

To further guide the selection of samples for sequencing, we examined the qPCR expression data for vGOIs (these data were also later used for RNA-Seq validation tests). For each vGOI we looked for patterns that identified samples with strong molecular responses to experimental treatments. This expression analysis pointed to the same key samples as the horticulture data for a global-scale gene expression analysis. For most vGOIs we observed dramatic contrasts in gene activity from TC-0 through TC-2 and between equivalent time points TE-1 and TC-2; for examples of this pattern see Fig. 3.

One vGOI of particular interest was a MDP0000150382, a UDP-glucosyltransferase similar to a gene that in several *Brassica* species is stress responsive (Rehman et al., 2018); this gene showed a dramatic induction during the first two weeks of storage that was reversed by 5 d of 20 °C warming (Fig. 3). Gene expression shifts and contrasts in samples taken later in the storage period for vGOIs were generally of lower magnitude indicating the earlier intermittent warming treatments, which were also most effective to reduce superficial scald (Figs. 1 and 2), likely represent important shifts in molecular responses related to disorder attenuation. Therefore, for RNA-Seq analysis we selected TC-0, TC-1, TC-2, and TE-1. We also included a fine time course at 24 h intervals during the initial warming treatment (T1.1–T1.5, with T1.5 = TE-1) (see Supplemental Fig. 1 for a sample summary).

3.3. RNA-Seq validation

The vGOIs (selected prior to sequencing) were used to validate our RNA-Seq count data. Generally, the qPCR estimates of gene expression were highly concordant with RNA-Seq estimates, though there were examples of disagreement between the technologies (Supplemental Table 1, Supplemental Fig. 5). We regressed the observations for each technology ($R^2 = 0.80$), as well as the means of observations ($R^2 = 0.90$). The increase in R^2 by regressing the means suggests technical rather than biological sources of variance. Our validation results generally agree with recent examples of apple transcriptome analysis (Busatto et al., 2018; Legay et al., 2015; Zermiani et al., 2015); we note that qPCR validation of RNA-Seq data in apple transcriptome analysis is not standardized, or even routinely conducted (Gapper et al., 2017). There is evidence that gene polymorphisms contribute to loss of signal in gene expression experiments (Lefever et al., 2013), such may be the case in cross-cultivar RNA-Seq experiments in apple (Hargarten et al., 2018). This likely contributes to the somewhat variable results of qPCR validation in the literature for cross-cultivar RNA-Seq experiments in apple, and what is presented here.

A principle component analysis (PCA) of count data indicated the main source of variance was experimental treatments and that variance between biological replicates was low (Supplemental Fig. 6). Concordant with this analysis was an assessment of the genes with the greatest variance between the control (TC-2) and the intermittently warmed experimental samples (TE-1) as these genes showed low variance among observations, but dramatic differences between treatments (Supplemental Fig. 7). Biological replicates for both TE-1 and TC-2 were highly correlated and a second PCA showed clear separation between these two samples with biological replicates clustering together (Supplemental Fig. 8).

3.4. Differential expression analysis of warmed vs. consistently cold fruit

Of primary interest was the set of differentially expressed genes (DEGs) between heavily symptomatic fruit that had been stored at a consistent 1 °C (TC-2) and fruit in which superficial scald was effectively reduced with a warming treatment (TE-1). As part of a quality control check, we examined the genes with the highest variance between these two sample groups. In addition to verifying that the sample treatments were the largest source of variance, it also revealed the most dramatic shifts in gene expression between consistently cold and intermittently warmed apple fruit. Of the 25 genes in this analysis,

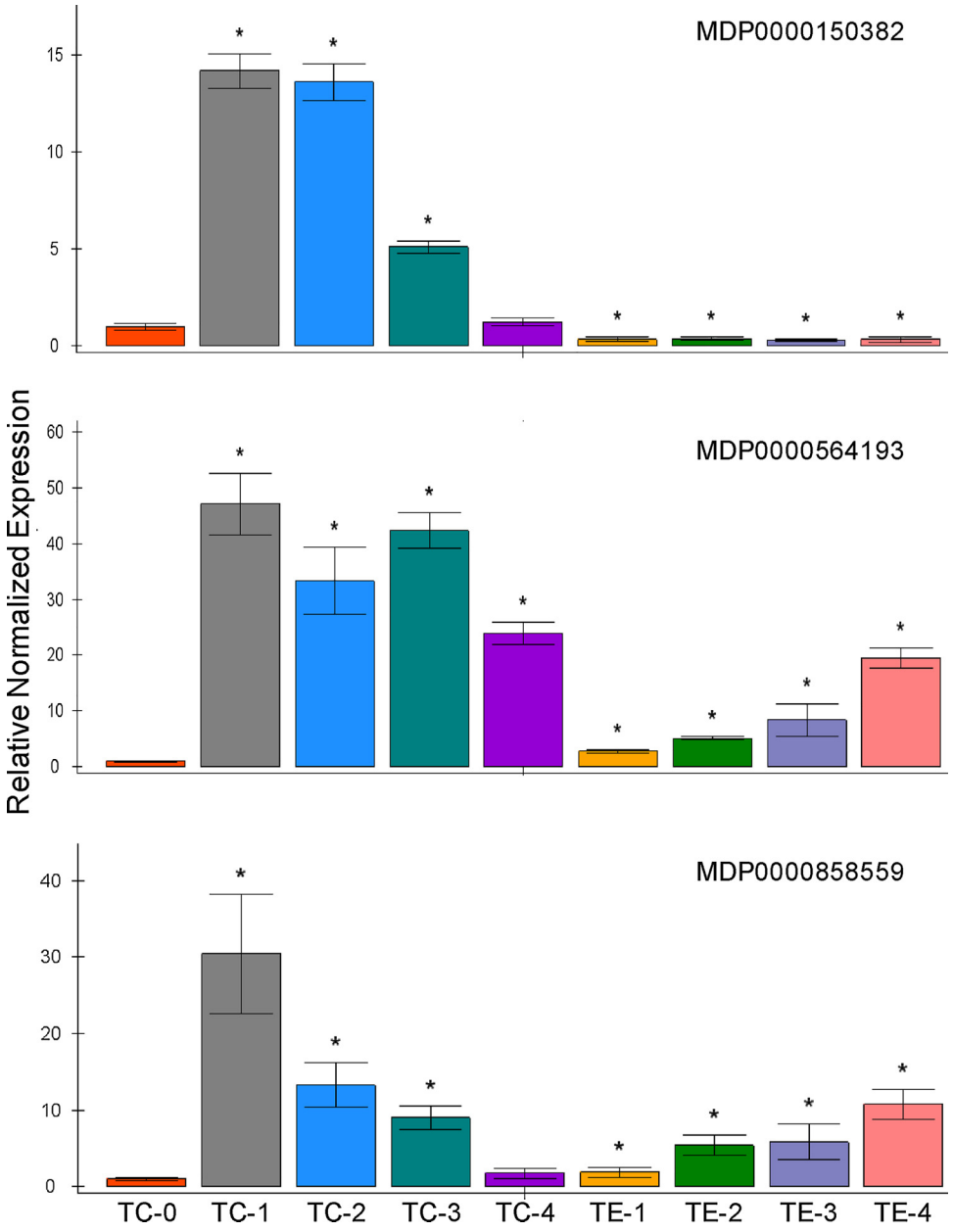

Fig. 3. Select vGOIs (3 of 15) showing representative large shifts in initial warming treatments compared to subsequent ones, highlighting TE-1 vs. TC-2 as a critical comparison for gene expression changes in response to intermittent warming. TC samples are a time course, beginning with harvest (TC-0) and then consistent chilling at 1 °C with sampling for RNA at one, two, four, and eight weeks (respective to TC-1, TC-2, TC-3, and TC-4). TE samples were chilled the same as TC samples, except they were intermittently warmed for 5 d at 20 °C at one, two, four, and eight weeks (respective to TE-1, TE-2, TE-3, and TE-4). Plots show relative normalized expression with SE. * significantly different ($p < 0.05$) from control (TC-0).

downregulated genes were far more common (~6:1) and showed a larger average fold change (1,165× vs. 102×) indicating that the warming event was characterized by a reversal trend for genes activated by chilling stress, vs. upregulation in response to warming. This pattern of reversal vs. induction by warming persisted especially for genes with fold changes > 2 (Supplemental Fig. 9).

The upregulated genes in this list were not functionally diverse, with three of four annotated as lipoxygenase and the fourth as a chaperon for heat tolerance (Supplemental Table 2). The *Arabidopsis* homologs (best hits to apple genes –apple v1.0 at phytozome.jgi.doe.gov & www.arabidopsis.org) of the 21 downregulated genes often were annotated as responsive to abiotic stimuli including cold stress, drought, heavy metal exposure, and oxidative stress. The encoded proteins include putative dehydrins, late embryogenesis abundant proteins, and peroxidases (Supplemental Table 2). A prominent feature in this analysis was a peroxidase and the most differentially expressed gene in the analysis (MDP0000611163; the *Arabidopsis thaliana* homolog AT5G06720 is annotated as responsive to oxidative stress). This peroxidase gene was upregulated ~125 fold in the first week of cold storage, and was downregulated ~4400 fold (almost to 0) after one week at 20 °C.

The pairwise differential expression analysis showed us the most treatment-responsive genes in our dataset, but discovering the top differential genes did little to enhance our view of superficial scald etiology and its prevention by intermittent warming. The top differential genes largely fell into categories that were concordant with our current understanding of the disorder physiology; superficial scald is a chilling and oxidative stress-related disorder (Lurie and Watkins, 2012) and lipoxygenases are induced by ethylene and active during apple fruit ripening (Contreras et al., 2016). The complete list of DEGs was massive at > 13,000 and parsing such a large list in a biologically relevant way was not feasible. We therefore dug deeper into the RNA-Seq data to find genes that were co-expressed using a network approach.

3.5. Network construction to discover co-expression modules correlated with warming

A co-expression network analysis finds genes that have highly

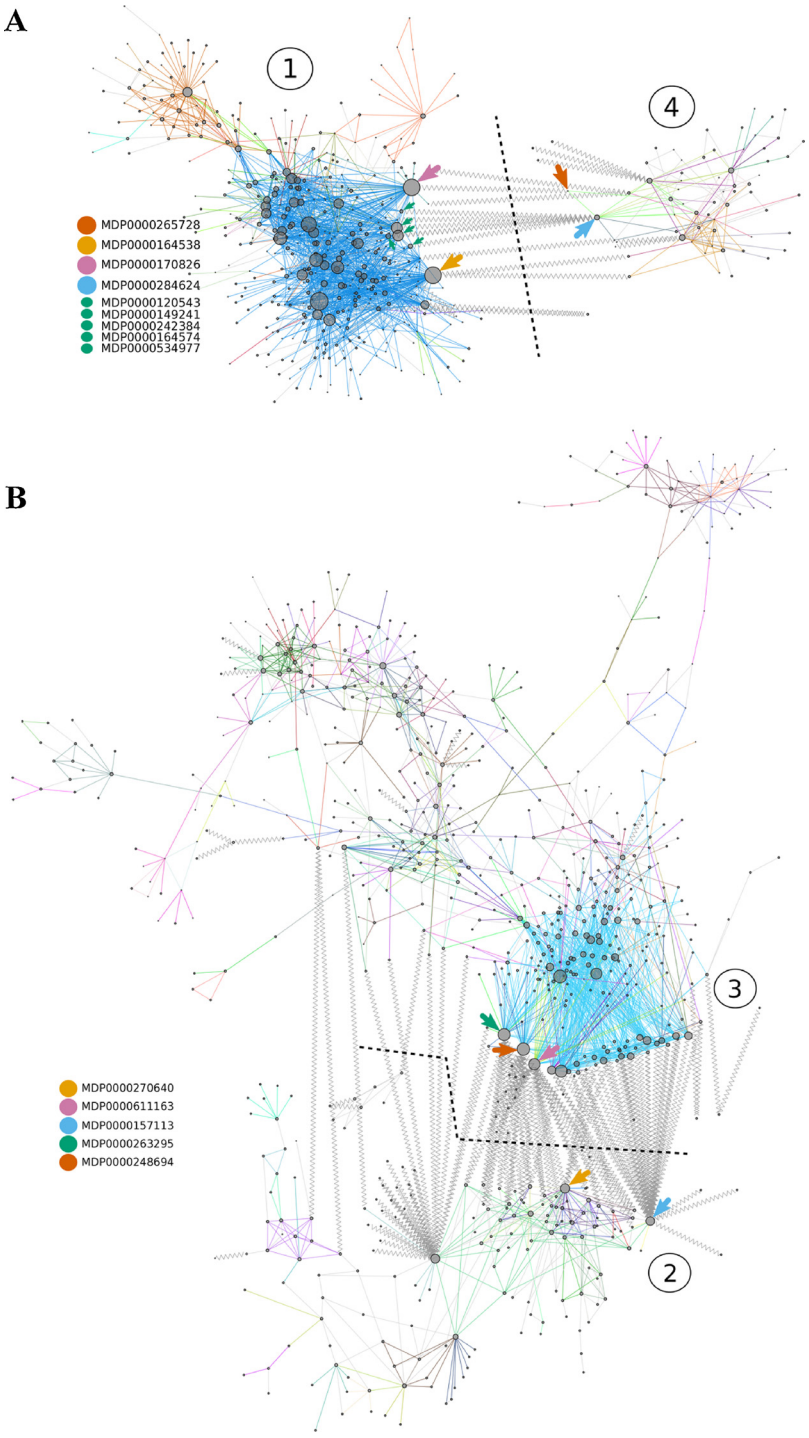

Fig. 4. A. Co-expression network modules 1 and 4 (displayed with a network topology emphasis). Edges (positive correlations, solid lines) are colored according to submodule identified using the linked communities approach. Genes connecting submodules are not necessarily mutually exclusive. Node size is specified by link degrees. Inverse correlations are indicated by gray zigzag lines and notable network features are indicated by colored arrows. The color of circles in the legend corresponds to the arrow colors and indicates the names of genes of interest. The dashed line indicates approximate module boundaries. **B. Co-expression network modules 2 and 3 (displayed with a network topology emphasis)**. Graphics follow Fig. 4A.

correlated activity – a guilt-by-association strategy to identify genes that operate together in processes of interest. In a forward genetics approach, we used a network analysis to discover collections of genes, or modules, that responded to the warming treatment in concert. Initially, using 'maSigPro', we clustered genes by expression for each of three time series into nine clusters. The coarse granularity of this approach, resulting in part from the coarse granularity of sampling, failed to identify lists of genes that were sufficiently large for functional enrichment analysis, or were too large to parse in a biologically relevant way.

Our next step was a refined network approach that used empirical evidence to specify finer cluster granularity and a strict correlation regression threshold for inclusion into the network. Beginning with all of the count data, and then refining network construction in part based on a regression with warming time (fine time course T1.1–1.5), the final network included 1307 nodes (genes) sorted into a mutually exclusive set of four modules with 25, 120, 33, and 14 submodules, respectively for modules 1 through 4 (Fig. 4A & B, see Supplemental File 3 for network file).

Of the 1307 genes in the network, ~75% (n = 965) were also present in the massive list of DEGs (n = 13,317), showing that co-regulated genes also tended to be differentially expressed in response to experimental treatments. The top 25 DEGs, except MDP0000611163, were not present in the network, perhaps due to their high variance between treatments and thus insufficient R^2 given our cutoff of > 0.9. To integrate our DE analysis with the network analysis we specified

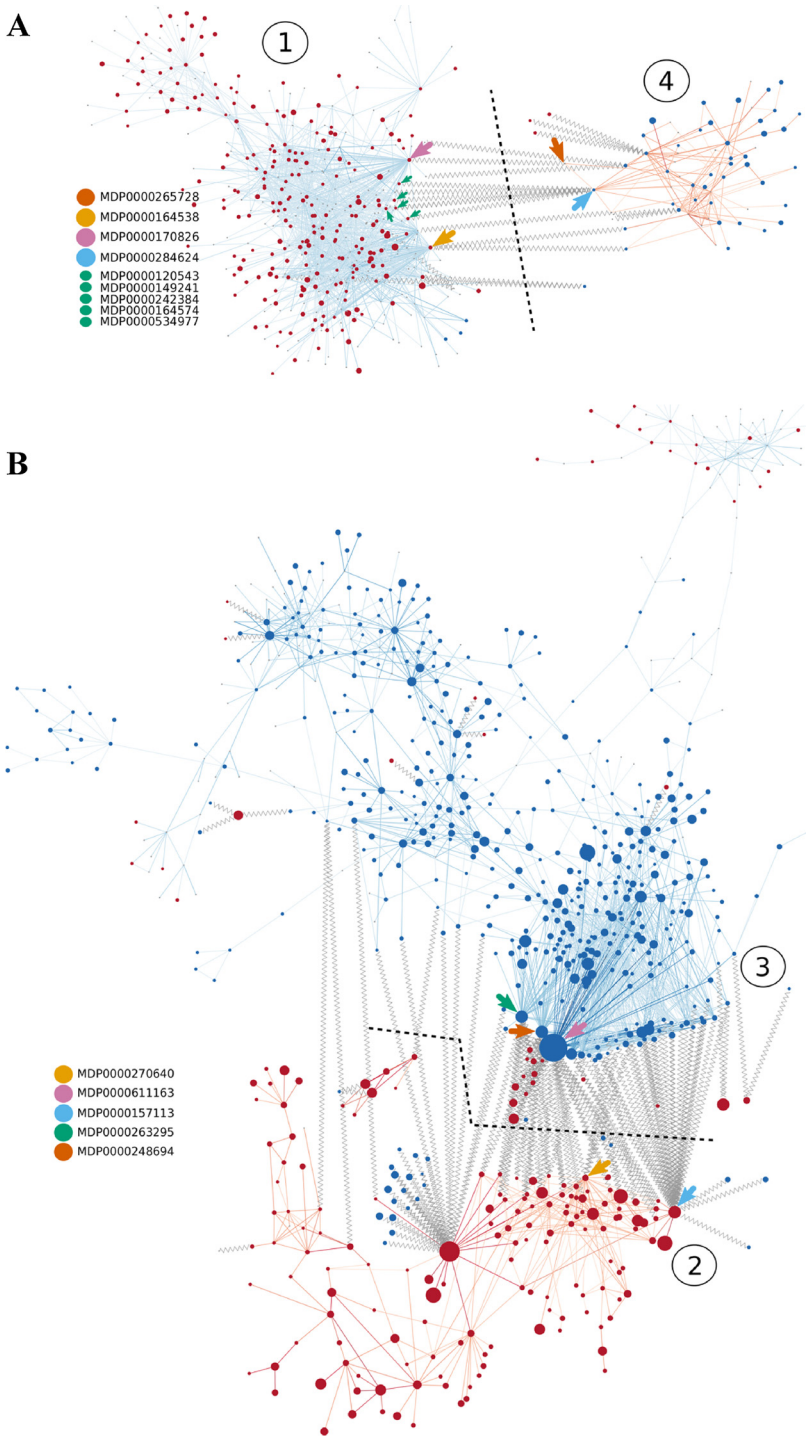

Fig. 5. A. Co-expression network modules 1 and 4 (displayed with a gene expression emphasis). Nodes, representing genes, are colored according to directionality of change between the TC-2 (control) and TE-1 (experimental) treatments, with blue indicating a negative fold change and red a positive fold change. Node size reflects the absolute magnitude of fold change. Edges are colored similarly to nodes and the color intensity of edges represents rates of change during intermittent warming, with more intense shades reflecting greater rates of change. Modules are identified with circled numbers and a dashed line indicates approximate module boundaries. Inverse correlations are indicated by gray zigzag lines, and notable network features are indicated by colored arrows. This module pair showed an expression pattern that was incongruent with the co-expression network analysis – down regulated genes were trending up during intermittent warming, and vice-versa. This was due to a rapid oscillation during the initial 24–48 h of warming. **B. Co-expression network modules 2 and 3 (displayed with a gene expression emphasis)**. Graphics follow Fig. 5A. This module pair showed an expression pattern that was congruent between the differential expression analysis and co-expression analysis - down regulated genes were trending down during intermittent warming, and vice-versa.

node size by magnitude of log2 fold change, and color by directionality of change (red for up and increasing and blue for down and decreasing). We used a similar scheme for edge color but with edge color intensity reflecting the magnitude of change (Fig. 5A & B).

The modules, although distinct, did have inverse relationships, creating the pairs (2 with 3, and 1 with 4) that persist for our presentation and subsequent discussion of their characteristic functional profiles. For modules 2 and 3, the correlation with warming time was congruent with the directionality of change for DEGs, that is, upregulated genes were positively correlated with warming time, and down regulated genes were negatively correlated with warming time (Fig. 5B). We observed the opposite directionality of fold change and correlation with warming time for modules 1 and 4; differentially up-regulated genes were negatively correlated with warming time and vice versa – opposite of modules 2 and 3.

As the network contains > 1000 nodes with complex relationships, we recommend viewing the network (Supplemental File 3) in Cytoscape, an open source platform for complex network analysis (http://www.cytoscape.org/). This allows viewers to search for apple gene IDs, learn about their functions, and easily interact with the network illustration. Additionally, we have provided gene lists (e.g. m1.GOI) that are compatible with the “Select Nodes – from ID list file” function of Cytoscape (See Supplemental File 2) to easily highlight genes of interest (GOIs).

3.6. Circumscription of genes of interest

To select GOIs for functional analysis we cross-referenced genes that were differentially expressed (FDR corrected $p < 0.01$, comparing TC-2 with TE-1, i.e. fruit that were consistently cold vs. fruit that were warmed during the cold storage period) with genes in the network, paying special attention to network topology. Because the network analysis circumscribed genes that were generally also DEGs, we used the four distinct modules as starting points and then added objective criteria to create gene lists for enrichment analysis.

For module 1, ~63% of the nodes belonged to a single submodule (See submodule SG01M0026 in Supplemental File 3). Because this submodule dominated module 1 topology (Supplemental Fig. 10), we selected these genes as list "Module 1 GOI" (m1.GOI, n = 270 genes). Module 4 was small (n = 47 genes, see SG04 in Supplemental File 3), with the fewest submodules (n = 14), yet a majority of genes (~65%) were DEGs – we chose all members of module 4 as list "Module 4 GOI" (m4.GOI, see Supplemental Fig. 10). The characteristic gene expression pattern of this module pair was that during the first 48 h of warming there was a rapid oscillation, showing a brief reversal of chilling-induced gene expression changes, with a return towards pre-warming levels (Fig. 6A & B).

Modules 2 and 3 (Supplemental Fig. 11) were larger and more complex yet seemed to be organized around a prominent feature: the MDP0000611163 gene (see arrows in Fig. 5B, Fig. 7A, and Supplemental Fig. 11).

We combined network topology around this feature (nodes with ≤3° of separation from MDP0000611163) with our list of DEGs to circumscribe upregulated genes thus defining list "Module 2 GOI" (m2.GOI. n = 97), and downregulated genes defining list "Module 3 GOI" (m3.GOI, n = 246) (see Supplemental File 2 for GOI lists). The characteristic gene expression pattern in this module pair was a simple but strong reversal (and slight overshot) of chilling induced gene expression changes that occurred during the first week of cold storage.

3.7. Functional enrichment of GOI

We determined the functional profiles of GOIs in co-expression modules by enrichment analysis of GO (www.geneontology.org) biological process (BP) and molecular function (MF) terms. Eight to sixteen BP terms and 12–19 MF terms were enriched in each GOI list. For m1.GOI (showing a brief increase in response to warming) the functional profile was dominated by amino acid metabolism and tRNA synthesis terms (Table 2).

Glycolysis and gluconeogenesis terms were also enriched. Together these signatures suggest an energetic response to intermittent warming that includes protein biosynthesis. Porphyrin and chlorophyll biosynthesis terms were overrepresented among m1.GOIs as well.

For m4.GOI (showing a brief decrease in response to warming) the functional profile was quite distinct from m1.GOI, including transferase, signaling, and transport terms (Table 3).

An interesting inverse link was discovered between a prominent but cryptic feature MDP0000170826 (IPR007650 – domain of unknown function, pink arrow Figs. 4A & 5 A) and an ABA receptor (MDP0000284624, blue arrow Figs. 4A & 5 A) via MDP0000265728 (with enriched GO term GO:0005992 "trehalose biosynthetic process", red arrow Figs. 4A & 5 A). Trehalose plays a diversity of roles in higher plants that are not completely understood but is part of cold stress responses (Lunn et al., 2014). Also enriched was the molecular function GO:0004402 "histone acetyltransferase activity" suggesting epigenetic modifications (Wakeel et al., 2018) may play a role in superficial scald. Another signature (combination of GO:0006887 – exocytosis, GO:0015969 – GTP metabolic process, and GO:0032312 regulation of (GO:0008060) ARF GTPase activity) is suggestive of suppression of auxin mediated exocytosis via downregulation of ARF GTPase activators (Yorimitsu et al., 2014) in warmed fruit.

The m3.GOIs showed large transcriptional changes that were characterized by a reversal of gene expression induced by chilling. The enrichment analysis (Table 4) showed that "protein ubiquitination" was a prominent biological process along with "glycolytic processes," suggesting an energetic response to cold characterized by protein turnover via the proteasome.

Also apparent were "thiamine and arginine biosynthetic processes" – arginine may have an indirect link to abiotic stress response as it is a precursor to NO production (Gupta et al., 2011), and thiamine has been shown to play a more direct role in oxidative stress response (Tunc-Ozdemir et al., 2009). Mitochondrial modifications were suggested by the enrichment of "mitochondrial fission" (GO:0000266) and "protein

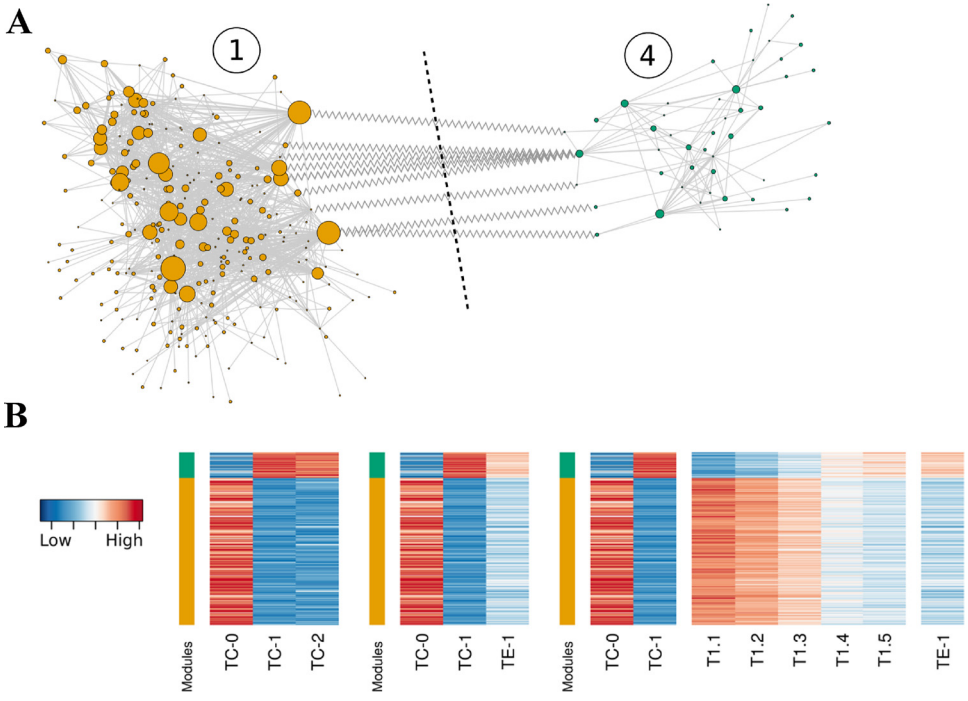

Fig. 6. A. Module 1 and 4 Genes of Interest (m1.GOI and m4.GOI). GOIs were selected from the network based on objective criteria that circumscribed genes that were highly correlated, differentially expressed and sufficiently numerous for enrichment analysis. The colored nodes correspond to colored bars in the associated heatmaps in Fig. 6B. The dashed indicates approximate module boundaries. **B. Expression patterns of m1.GOI and m4.GOI**. Gene expression patterns of control fruit (TC-0, TC-1, TC-2), intermittently warmed fruit (TC-0, TC-1, TE-1) and the 24 h interval time course (TC-0, TC-1, T1.1, T1.2, T1.3, T1.4, T1.5/TE-1) during warming. The colored bars correspond to the modules shown in Fig. 6A. The characteristic pattern of this module pair is the rapid oscillation of expression that returns towards pre-warming (TC-1) levels.

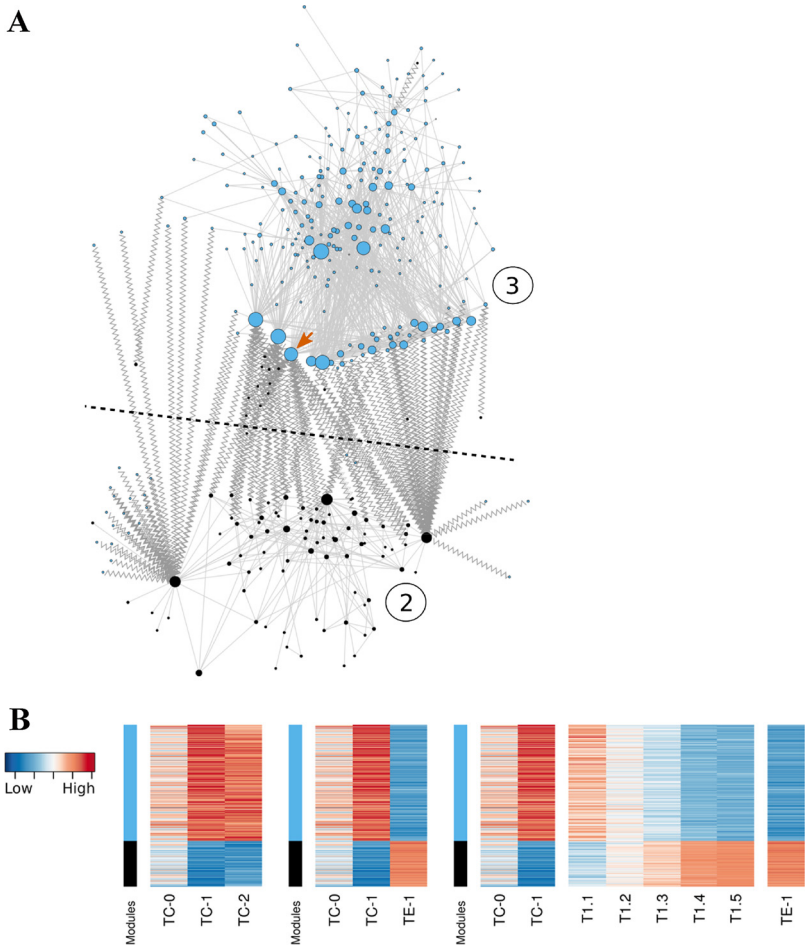

Fig. 7. A. Module 2 and 3 Genes of Interest (m1.GOI and m4.GOI). Graphics follow Fig. 6A. The colored nodes correspond to colored bars in the associated heatmaps in Fig. 7B. MDP611163 indicated by the orange arrow. **B. Expression patterns of m2.GOI and m3.GOI**. Graphics follow Fig. 6B. The characteristic pattern of this module pair is the recovery of gene expression through the time-series T1.1-T1.5/TE-1 towards, and then slightly past, at-harvest levels in sample TC-0. This module pair is distinct form the other pair in that the transition from TC-1 to TE-1 is a simple reversal back to at-harvest (TC-0 vs. T1.2 and T1.3) levels, then a slight overshot.

import into the mitochondrial inner membrane" (GO:0045039) terms. The latter term was associated with a gene (*Arabidopsis thaliana* homolog AT2G29530, https://www.arabidopsis.org/) that may encode a novel chaperone receptor in the chloroplast (MDP0000204238).

The functional enrichment analysis of m2.GOI, a module that showed a reversal of gene suppression in response to chilling, revealed several GO terms associated with metabolism, and two related to response to heat (Table 5).

GO biological process term (GO:0055114) "oxidation-reduction process" was strongly enriched and represented by diverse processes including antioxidant biosynthesis (MDP0000806502), carotenoid biosynthesis (MDP0000221455, MDP0000278241, MDP0000225539, MDP0000235597) and chloroplast-localized lipoxygenase activity (MDP0000281525).

3.8. Prominent network features

Broad patterns in the network were useful to identify groups of GOIs, but individual GOIs were easily highlighted based on network context. Criteria include prominent network positions and connections to genes that were differentially expressed or had interesting biological functions. For the module 2–3 pair, network topology revealed inverse correlations between highly correlated nodes in the module pair. These include the prominent peroxidase discussed above (MDP0000611163; Fig. 4B and 5 B pink arrow) that had first degree connections in both modules. Potassium channels MDP0000248694 (red arrow Fig. 4B and 5B) and MDP0000263295 (green arrow Fig. 4B and 5 B) both are annotated as a Shaker-type family outward-rectifying K^+ channels (Phytozome best *Arabidopsis* hit AT3G02850) that are potentially modulated by ABA (www.arabidopsis.org).

Another prominent network feature was a highly connected node in module 2 (Fig. 4B and 5 B, orange arrow, MDP0000270640). This is a 14-3-3 protein with a first-degree connection to MDP0000611163. 14-3-3 proteins have complex roles in plant signal transduction that are incompletely understood (Camoni et al., 2018). Our analyses suggest an important role for this gene as it is differentially expressed in a key comparison, and an organizing feature of a major co-expression module with an inverse relationship to an organizing feature of another major module. The closest *Arabidopsis* homolog for this 14-3-3 gene (AT1G34760) has been shown to stabilize 1-aminocyclopropane-1-carboxylate synthase (ACS), the enzyme catalyzing the rate limiting step in ethylene biosynthesis (Yoon and Kieber, 2013). The upregulation of this gene is consistent with enhanced ripening via warming and the elevated levels of ethylene we detected in warmed fruit.

Finally in module 2, a cationic amino acid transporter (MDP0000157113, CAT1; Fig. 4B and 5 B, blue arrow) is inversely correlated with 27 genes in module 3, the most prominent example of an inverse relationship in the network. Overexpression of the *Arabidopsis* homolog (AT4G21120) confers enhanced resistance to *Pseudomonas* (Yang et al., 2014), but its role in response to abiotic stress is unclear, though growing evidence suggests crosstalk between biotic and abiotic stress signaling pathways, especially in earlier response phases (Gassmann et al., 2016).

In the other module pair, 1 and 4, the inverse relationship was less dramatic, but did seem to organize around a small number of features. A PYL9/RCAR gene (ABA receptor family gene in module 4, MDP0000284624, Fig. 4A and 5 A, blue arrow) was inversely correlated with five differentially expressed genes in module 1 (Fig. 4A and 5 A, small green arrows). These included MDP0000120543, a glucosyltransferase (*Arabidopsis* homolog Quasimodo1), that regulates calcium

Table 2
Module 1 Gene of Interest functional enrichment analysis results. List of significantly enriched GO Terms; Ontology categories- BP: Biological Process, MF: Molecular Function.

Term	Fisher's p-value	Ontology	Description
GO:0006418	1.98E-07	BP	tRNA aminoacylation for protein translation
GO:0009089	7.88E-05	BP	lysine biosynthetic process via diaminopimelate
GO:0006526	0.0002	BP	arginine biosynthetic process
GO:0015995	0.0002	BP	chlorophyll biosynthetic process
GO:0006431	0.0009	BP	methionyl-tRNA aminoacylation
GO:0006094	0.0011	BP	gluconeogenesis
GO:0043039	0.0020	BP	tRNA aminoacylation
GO:0006434	0.0028	BP	seryl-tRNA aminoacylation
GO:0015746	0.0039	BP	citrate transport
GO:0006096	0.0044	BP	glycolysis
GO:0006568	0.0044	BP	tryptophan metabolic process
GO:0008652	0.0055	BP	cellular amino acid biosynthetic process
GO:0006435	0.0064	BP	threonyl-tRNA aminoacylation
GO:0009408	0.0064	BP	response to heat
GO:0006438	0.0079	BP	valyl-tRNA aminoacylation
GO:0006779	0.0095	BP	porphyrin biosynthetic process
GO:0004812	1.99E-07	MF	aminoacyl-tRNA ligase activity
GO:0004347	8.13E-05	MF	glucose-6-phosphate isomerase activity
GO:0000166	8.63E-05	MF	nucleotide binding
GO:0008836	0.0003	MF	diaminopimelate decarboxylase activity
GO:0004825	0.0009	MF	methionine-tRNA ligase activity
GO:0004055	0.0012	MF	argininosuccinate synthase activity
GO:0016876	0.0014	MF	ligase activity, forming aminoacyl-tRNA and related compounds
GO:0004746	0.0016	MF	riboflavin synthase activity
GO:0004828	0.0028	MF	serine-tRNA ligase activity
GO:0015137	0.0039	MF	citrate transmembrane transporter activity
GO:0004829	0.0064	MF	threonine-tRNA ligase activity
GO:0004832	0.0079	MF	valine-tRNA ligase activity

Table 4
Module 3 Gene of Interest functional enrichment analysis results. List of significantly enriched GO Terms; Ontology categories- BP: Biological Process, MF: Molecular Function.

Term	Fisher's p-value	Ontology	Description
GO:0006096	0.000038	BP	glycolytic process
GO:0016567	0.0015	BP	protein ubiquitination
GO:0006368	0.0048	BP	transcription elongation from RNA polymerase II promoter
GO:0042450	0.0099	BP	arginine biosynthetic process via ornithine
GO:0000266	0.0148	BP	mitochondrial fission
GO:0045039	0.0196	BP	protein import into mitochondrial inner membrane
GO:0016570	0.024	BP	histone modification
GO:0009228	0.0484	BP	thiamine biosynthetic process
GO:0004719	0.000064	MF	protein-L-isoaspartate (D-aspartate) O-methyltransferase activity
GO:0019905	0.000064	MF	syntaxin binding
GO:0004743	0.0012	MF	pyruvate kinase activity
GO:0030955	0.0012	MF	potassium ion binding
GO:0030170	0.0036	MF	pyridoxal phosphate binding
GO:0008440	0.0093	MF	inositol-1,4,5-trisphosphate 3-kinase activity
GO:0045131	0.0093	MF	pre-mRNA branch point binding
GO:0004056	0.0093	MF	argininosuccinate lyase activity
GO:0016706	0.0139	MF	Oxidoreductase activity, acting on paired donors, with incorporation or reduction of molecular oxygen
GO:0008253	0.0185	MF	5'-nucleotidase activity
GO:0051536	0.023	MF	iron-sulfur cluster binding
GO:0000287	0.0321	MF	magnesium ion binding
GO:0009916	0.0322	MF	alternative oxidase activity
GO:0008883	0.0322	MF	glutamyl-tRNA reductase activity
GO:0005216	0.0385	MF	ion channel activity
GO:0004618	0.0457	MF	phosphoglycerate kinase activity
GO:0000049	0.0457	MF	tRNA binding
GO:0008725	0.0457	MF	DNA-3-methyladenine glycosylase activity
GO:0051082	0.0468	MF	unfolded protein binding

signaling during drought and salt stress in *Arabidopsis,* evidenced in part by lack of stomatal closure in response to ABA in the mutant (Zheng et al., 2016). Also included were two genes with high degrees of connectivity in the network (> 40 link degrees): MDP0000149241 and MDP0000242384, a threonyl tRNA synthase and thymidylate synthase, respectively. The former is most notably a mobile transcript that is targeted to both the mitochondrion and chloroplast (Thieme et al., 2015) and the latter is differentially expressed via cell cycle regulation

Table 3
Module 4 Gene of Interest functional enrichment analysis results. List of significantly enriched GO Terms; Ontology categories- BP: Biological Process, MF: Molecular Function.

Term	Fisher's p-value	Ontology	Description
GO:0009435	1.92E-06	BP	NAD biosynthetic process
GO:0015969	0.0013	BP	guanosine tetraphosphate metabolic process
GO:0006887	0.0014	BP	exocytosis
GO:0006221	0.0027	BP	pyrimidine nucleotide biosynthetic process
GO:0006857	0.0061	BP	oligopeptide transport
GO:0006855	0.0063	BP	drug transmembrane transport
GO:0005992	0.0066	BP	trehalose biosynthetic process
GO:0032312	0.0077	BP	regulation of ARF GTPase activity
GO:0008987	1.60E-07	MF	quinolinate synthetase A activity
GO:0033926	0.0014	MF	glycopeptide alpha-N-acetylgalactosaminidase activity
GO:0003883	0.0017	MF	CTP synthase activity
GO:0016857	0.0019	MF	racemase and epimerase activity, acting on carbohydrates and derivatives
GO:0004402	0.0022	MF	histone acetyltransferase activity
GO:0003712	0.0038	MF	transcription cofactor activity
GO:0005198	0.0039	MF	structural molecule activity
GO:0004842	0.0042	MF	ubiquitin-protein ligase activity
GO:0015238	0.0063	MF	drug transmembrane transporter activity
GO:0015297	0.0063	MF	antiporter activity
GO:0016706	0.0072	MF	oxidoreductase activity, acting on paired donors, with incorporation or reduction of molecular oxygen, 2-oxoglutarate as one donor, and incorporation of one atom each of oxygen into both donors
GO:0008060	0.0077	MF	ARF GTPase activator activity
GO:0016758	0.0089	MF	transferase activity, transferring hexosyl groups

Table 5
Module 2 Gene of Interest functional enrichment analysis results. List of significantly enriched GO Terms; Ontology categories- BP: Biological Process, MF: Molecular Function.

Term	Fishers p-val	Ontology	Description
GO:0055114	0.0001	BP	oxidation-reduction process
GO:0009408	0.0023	BP	response to heat
GO:0006559	0.0069	BP	L-phenylalanine catabolic process
GO:0009958	0.0093	BP	positive gravitropism
GO:0006570	0.0161	BP	tyrosine metabolic process
GO:0005975	0.0207	BP	carbohydrate metabolic process
GO:0030259	0.0275	BP	lipid glycosylation
GO:0009072	0.0285	BP	aromatic amino acid family metabolic process
GO:0006633	0.0361	BP	fatty acid biosynthetic process
GO:0010309	0.000025	MF	acireductone dioxygenase [iron(II)-requiring] activity
GO:0005506	0.0001	MF	iron ion binding
GO:0003995	0.00063	MF	acyl-CoA dehydrogenase activity
GO:0016705	0.00298	MF	oxidoreductase activity, acting on paired donors, with incorporation or reduction of molecular oxygen
GO:0008233	0.00405	MF	peptidase activity
GO:0004411	0.00618	MF	homogentisate 1,2-dioxygenase activity
GO:0020037	0.00692	MF	heme binding
GO:0045145	0.00823	MF	single-stranded DNA 5'-3' exodeoxyribonuclease activity
GO:0016787	0.00826	MF	hydrolase activity
GO:0003868	0.01232	MF	4-hydroxyphenylpyruvate dioxygenase activity
GO:0004106	0.01232	MF	chorismate mutase activity
GO:0000062	0.01842	MF	fatty-acyl-CoA binding
GO:0031072	0.02449	MF	heat shock protein binding
GO:0004177	0.04642	MF	aminopeptidase activity

and is primarily expressed in meristems (Maniga et al., 2017). Another is a putative cytochrome b5 reductase (MDP0000164574) that has been shown in *Arabidopsis* to increase fatty acid levels (Oh et al., 2016); these compounds are known to stabilize membranes during chilling stress and have been reported to change in apple fruit responding to chilling stress (Busatto et al., 2018; Gapper et al., 2017). The fifth is a putative chaperonin (MDP0000534977), and although previous work has not supported a response to ABA signaling (Zhang et al., 2013) our analysis shows a clear and strong inverse correlation with the aforementioned ABA receptor gene.

Two other prominent features were present in the module 1, 4 pair, but had little or no functional annotation, including one gene annotated only with an InterPro Domain of unknown function (DUF581 – MDP0000170826- pink arrow Fig. 4A and 5 A), another only with nucleic acid and zinc binding domains (MDP0000164538 – orange arrow Fig. 4A and 5 A). MDP0000170826, as previously discussed, is inversely linked via MDP0000265728 to the ABA receptor (MDP000284624), suggesting a role as a signaling intermediate in ABA hormone signaling during intermittent warming of apple fruit that may involve this protein of unknown function. The Arabidopsis homolog of MDP0000170826 is annotated as senescence-associated and has been implicated in abiotic stress responses (Luhua et al., 2013).

4. Discussion

4.1. Intermittent warming during cold storage influences apple fruit quality

Intermittent warming of cold-stored fruit to influence fruit quality in the postharvest period is ostensibly compliant with crop protectant-limited production systems. Here we have shown, consistent with a previous report (Watkins et al., 1995), that the intermittent warming of 'Granny Smith' apple fruit reduced superficial incidence and scald severity. In this study it was as effective as DPA applied at the same time as the warming treatment, however DPA treatment at harvest was marginally more effective at reducing scald compared to DPA treatment after 1 week cold storage. Overall fruit quality was low in this experiment because of prolonged air-storage designed to allow scald development, though fruit quality did vary as expected with warmed fruit, indicated by ripening, lower firmness, and higher ethylene content relative to un-warmed fruit. As previously discussed, there are several ways to control superficial scald, and many factors in the postharvest storage environment can be manipulated to influence outcomes – exactly how these factors interact with intermittent warming regimes is largely unknown, as are the molecular signatures produced by these possible interactions.

4.2. Co-expression analysis reveals distinct responses classes of apple fruit to warming

Our GOIs encode functionally distinct transcriptional responses of 'Granny Smith' apple fruit to intermittent warming. Substantial fold changes in gene expression during the first week of cold storage were a shared characteristic of all GOIs, but how gene expression changed in response to warming was highly distinct – one class showed a complete and sharp reversal of patterns emerging from harvest through one week of cold storage. The other showed a rapid oscillation, with gene expression increasing or decreasing and then returning to near pre-warming levels by the end of the warming treatment. Of interest was a striking inverse correlation between pairs of GOI groups, suggesting regulatory mechanisms with coordinated signaling cross-talk, that resulted in divergent patterns of expression for each group of GOIs.

The GOIs that showed a simple reversal trend (m2.GOI and m3.GOI) returned to and then slightly overshot *at-harvest* levels of expression. This may suggest recovery from mild chilling occurring at night around the time of harvest. This contrasts with the genes (m1.GOI and m4.GOI) that showed an oscillation with a return to *prewarming* levels, not *at-harvest* levels. This suggests the module 1–4 pair represents a response specifically to the warming treatment.

4.3. Warming causes a reversal of stress responsive gene expression in chilled fruit

A dominant signature of intermittently warmed apple fruit was a reversal of abiotic stress induced genes, which correlates with a significant reduction in the chilling-related apple fruit disorder superficial scald. The most prominent among these signatures was the > 100 fold induction of a peroxidase gene during one week of cold storage that was reduced > 4000 fold to nearly 0 after five days of warming. In a similar previous study the induction of this gene was prevented by blocking ethylene action with 1-MCP, but was unaffected by DPA, although both treatments effectively controlled scald (Gapper et al., 2017) supporting distinct mechanisms of scald prevention for each compound. This peroxidase was also an organizing feature of a co-expression network that revealed ubiquitin mediated protein turnover, mitochondrial modification, and thiamine biosynthesis as a part of the mechanism to prevent scald. Interestingly arginine biosynthesis was also reversed by warming, perhaps reducing flux into the nitric oxide (NO) pathway. Apple fruit in storage does produce NO, and levels vary during storage (unpublished) though the role of arginine biosynthesis, and specifically as it relates to NO production, is unclear in superficial scald etiology.

The genes induced by warming in module 2 were tightly correlated with abiotic stress gene activity that was reversed by warming. These are largely consistent with enhanced ripening of climacteric fruit via warming, including lipoxygenases and heat shock proteins. A 14-3-3 protein, the Arabidopsis homolog known to stabilize ACS in the ethylene biosynthesis pathway (Yoon and Kieber, 2013), was a notable network feature. In addition to a putative role in promoting ethylene biosynthesis for this particular 14-3-3 protein, there is evidence that 14-3-3 proteins act generally as signaling adapters that can integrate environmental cues with cell signaling (Comparot et al., 2003; Denison

et al., 2011; Jaspert et al., 2011). This highlights this gene of interest – perhaps as a genetic link between the fruit storage environment and control of ripening.

Two Shaker type potassium channels induced by chilling stress were also downregulated by warming. Potassium channels in this family are involved in ABA mediated stomatal closure, but also in potassium efflux out of stelar root cells into the xylem (Johansson et al., 2006). Potassium level in both fruit and leaves is positively correlated with scald susceptibility (Emongor et al., 1994), though the specific role for potassium in superficial scald is unclear. The expression of these K^+ channels does correspond to another feature in our co-expression network - an ABA receptor protein PYL9 - which is interesting because shaker-type potassium channels are known to be ABA responsive genes.

4.4. Network topology and fine sampling point to ABA signaling during warming

A surprising outcome of the co-expression analysis was the discovery of differentially expressed genes that showed a rapid oscillation, returning to near pre-warming levels after approximately five days, the same amount of warming time required to mitigate scald in 'Granny Smith' apple fruit. These changes were characterized by an induction of translation machinery, and a brief down regulation of an ABA receptor, epigenetic modification machinery, and genes involved in auxin mediated exocytosis. The inverse correlations show fatty acid metabolism, calcium signaling, and cell cycle regulation are all upregulated by warming and linked to downregulation of an ABA receptor. How these correlated processes interact in the context of a necrotic peel disorder is unclear, though the particular ABA receptor identified in our analysis, PYL9, when activated by ABA can promote programmed cell death (i.e. senescence) (Zhao et al., 2016). The response to ABA via PYL9 is dependent on tissue context, resulting in strong dormancy of young leaves and meristems, while promoting senescence in older tissues, a phenotype the authors point out is easily confused with drought sensitivity (Zhao et al., 2016). This observation may provide a clue to superficial scald etiology as fruit maturity is a crucial factor in susceptibility to this disorder (Lurie and Watkins, 2012).

Apple fruit metabolism leading to scald symptom development has not been definitively described. One hypothesis is that plastids are destabilized by chilling stress, leading to oxidative stress that is quenched by phenolic antioxidants resulting in tissue browning (Busatto et al., 2018). Another is that superficial scald lesions result from programmed cell death in the epidermis; the long period between injury and symptom development, plus shifts in the metabolome and transcriptome suggest an active process rather than passive browning of oxidized, dead tissue (Gapper et al., 2017). Consistent with both hypotheses, our results show recovery from oxidative stress that includes fatty acid metabolism, organellar modifications, and antioxidant biosynthesis. However, our results also suggest recovery from the injury that leads to scald is an energetically active process involving proteasome mediated protein turnover and new protein synthesis. Plus, warming of fruit induced highly dynamic transcriptional responses that include downregulation of PYL9, an ABA receptor that has been shown to promote programmed cell death during abiotic stress (Zhao et al., 2016). This receptor was inversely correlated with expression of a cell-cycle regulated gene (programmed cell death is the final phase of the cell cycle) and a senescence-associated gene. These results support the hypothesis that superficial scald etiology includes activation of programmed cell death.

4.5. Genes involved in recovery from a chilling stress that causes scald

We have circumscribed candidate genes with activity in response to warming that makes them good candidates for exploring the molecular mechanisms of scald prevention by intermittent warming. This is because their activity is tightly correlated (both positively and negatively) with warming time sufficient to prevent scald. The fine scale network analysis revealed ostensibly warming-specific transcriptional responses to warming that within five days returned to near pre-warming levels. That five days of warming is sufficient for superficial scald reduction in 'Granny Smith' apples (in our experiment, and previously reported (Watkins et al., 1995)) presents an intriguing possibility – among these genes are those interposed between abiotic stress and physiological changes in apple peel that lead to scald. Discernment of molecular mechanisms of scald will require additional years of data with 'Granny Smith' apples as well as experiments with other cultivars like Fuji that have a similar warming requirement, but a different window of warming efficacy (Lu et al., 2011).

5. Conclusion

Our transcriptome analysis of intermittently warmed 'Granny Smith' apple fruit has revealed molecular responses of apple fruit to changes in temperature in the postharvest period. A strength of this work is the examination of molecular responses produced by temperature alone, without crop protectants or modified atmosphere, providing a baseline to explore the interaction of postharvest treatments with storage temperatures. The fine-grained co-expression analysis revealed highly dynamic responses of 'Granny Smith' apple fruit on the order of hours that influenced fruit quality months later in cold storage, offering a glimpse into signaling events that mediate these processes. The deployment of new postharvest technologies and new apple cultivars with desirable postharvest traits depends on detailed knowledge of the molecular mechanisms of this disorder. The key result from this study is the identification of candidate genes for future work aimed at unraveling the genetic basis of complex traits that influence superficial scald.

Funding

This work was supported by the Washington Tree Fruit Research Commission project#TR-17-100A and the U.S. Department of Agriculture.

Acknowledgements

The excellent technical support provided by Janie Countryman is gratefully acknowledged.

Appendix A. Supplementary data

Supplementary material related to this article can be found, in the online version, at doi:https://doi.org/10.1016/j.postharvbio.2018.09.016.

References

Biernacki, C., Celeux, G., Govaert, G., Langrognet, F., 2006. Model-based cluster and discriminant analysis with the MIXMOD software. Comput. Stat. Data Anal. 51 (2), 587–600. https://doi.org/10.1016/j.csda.2005.12.015.

Bolger, A.M., Lohse, M., Usadel, B., 2014. Trimmomatic: a flexible trimmer for Illumina sequence data. Bioinformatics 30, 2114–2120. https://doi.org/10.1093/bioinformatics/btu170.

Bramlage, W.J., Meir, S., 1990. Chilling injury of crops of temperate origin. In: Wang, C.Y. (Ed.), Chilling Injury of Horticultural Crops. CRC Press, Inc, Boca Raton, Florida, pp. 37–69.

Busatto, N., Farneti, B., Commisso, M., Bianconi, M., Iadarola, B., Zago, E., Ruperti, B., Spinelli, F., Zanella, A., Velasco, R., Ferrarini, A., Chitarrini, G., Vrhovsek, U., Delledonne, M., Guzzo, F., Costa, G., Costa, F., 2018. Apple fruit superficial scald resistance mediated by ethylene inhibition is associated with diverse metabolic processes. Plant J. 93 (2), 270–285. https://doi.org/10.1111/tpj.13774.

Camoni, L., Visconti, S., Aducci, P., Marra, M., 2018. 14-3-3 proteins in plant hormone signaling: doing several things at once. Front. Plant Sci. 9, 1–8. https://doi.org/10.3389/fpls.2018.00297.

Comparot, S., Lingiah, G., Martin, T., 2003. Function and specificity of 14-3-3 proteins in the regulation of carbohydrate and nitrogen metabolism. J. Exp. Bot. 54 (382), 595–604. https://doi.org/10.1093/jxb/erg057.

Conesa, A., Nueda, M.J., (2017) maSigPro: Significant gene expression profile differences in time course gene expression data. R package version 1.50.0. https://rdrr.io/bioc/maSigPro/, Bioconductor, http://bioinfo.cipf.es/.
Contreras, C., Tjellström, H., Beaudry, R.M., 2016. Relationships between free and esterified fatty acids and LOX-derived volatiles during ripening in apple. Postharvest Biol. Technol. 112, 105–113. https://doi.org/10.1016/j.postharvbio.2015.10.009.
Daccord, N., Celton, J.-M., Linsmith, G., Becker, C., Choisne, N., Schijlen, E., van de Geest, H., Bianco, L., Micheletti, D., Velasco, R., Pierro, E., Gouzy, J., Rees, J.D.G., Guérif, P., Muranty, H., Durel, C.-E., Laurens, F., Lespinasse, Y., Gaillard, S., Aubourg, S., Quesneville, H., Weigel, D., van de Weg, E., Troggio, M., Bucher, E., 2017. High-quality *de novo* assembly of the apple genome and methylome dynamics of early fruit development. Nat. Genet. 49 (7), 1099–1106. https://doi.org/10.1038/ng.3886.
Denison, F.C., Paul, A.-L., Zupanska, A.K., Ferl, R.J., 2011. 14-3-3 proteins in plant physiology. Semin. Cell Dev. Biol. 22 (7), 720–727. https://doi.org/10.1016/j.semcdb.2011.08.006.
Emongor, V.E., Murr, D.P., Lougheed, E.C., 1994. Preharvest factors that predispose apples to superficial scald. Postharvest Biol. Technol. 4 (4), 289–300. https://doi.org/10.1016/0925-5214(94)90040-X.
Ficklin, S., Shealy, B., 2016. SystemsGenetics/KINC.R. GitHub. https://github.com/SystemsGenetics/KINC.
Ficklin, S.P., Dunwoodie, L.J., Poehlman, W.L., Watson, C., Roche, K.E., Feltus, F.A., 2017. Discovering condition-specific gene co-expression patterns using gaussian mixture models: aa cancer case study. Sci. Rep. 7 (1), 1–11. https://doi.org/10.1038/s41598-017-09094-4.
Gapper, N.E., Hertog, M.L., Lee, J., Buchanan, D.A., Leisso, R.S., Fei, Z., Qu, G., Giovannoni, J.J., Johnston, J.W., Schaffer, R.J., Nicolaï, B.M., Mattheis, J.P., Watkins, C.B., Rudell, D.R., 2017. Delayed response to cold stress is characterized by successive metabolic shifts culminating in apple fruit peel necrosis. BMC Plant Biol. 17 (1), 1–18. https://doi.org/10.1186/s12870-017-1030-6.
Gassmann, W., Appel, H.M., Oliver, M.J., 2016. The interface between abiotic and biotic stress responses. J. Exp. Bot. 67 (7), 2023–2024. https://doi.org/10.1093/jxb/erw110.
Gibson, S.M., Ficklin, S.P., Isaacson, S., Luo, F., Feltus, F.A., Smith, M.C., 2013. Massive-scale gene co-expression network construction and robustness testing using random matrix theory. PLoS One 8 (2), e55871. https://doi.org/10.1371/journal.pone.0055871.
Granatstein, D., Kirby, E., Ostenson, H., Willer, H., 2016. Global situation for organic tree fruits. Sci. Hortic. 208, 3–12. https://doi.org/10.1016/j.scienta.2015.12.008.
Gupta, K.J., Fernie, A.R., Kaiser, W.M., van Dongen, J.T., 2011. On the origins of nitric oxide. Trends Plant Sci. 16 (3), 160–168. https://doi.org/10.1016/j.tplants.2010.11.007.
Hargarten, H.L., Waliullah, S., Kalcsits, L., Honaas, L.A., 2018. Leveraging transcriptome data for enhanced gene expression analysis in apple. J. Am. Soc. Hortic. Sci. 143 (5), 333–346. https://doi.org/10.21273/JASHS04424-18.
Honaas, L., Kahn, E., 2017. A practical examination of RNA isolation methods for European pear (*Pyrus communis*). BMC Res. Notes 10 (1), 1–8. https://doi.org/10.1186/s13104-017-2564-2.
Huelin, F.E., Coggiola, I.M., 1970. Superficial scald, a functional disorder of stored apples. V.—oxidation of α-farnesene and its inhibition by diphenylamine. J. Sci. Food Agric. 21 (1), 44–48. https://doi.org/10.1002/jsfa.2740210113.
Jaspert, N., Throm, C., Oecking, C., 2011. *Arabidopsis* 14-3-3 proteins: fascinating and less fascinating aspects. Front. Plant Sci. 2, 1–8. https://doi.org/10.3389/fpls.2011.00096.
Johansson, I., Wulfetange, K., Porée, F., Michard, E., Gajdanowicz, P., Lacombe, B., Sentenac, H., Thibaud, J.B., Mueller-Roeber, B., Blatt, M.R., Dreyer, I., 2006. External K+ modulates the activity of the *Arabidopsis* potassium channel SKOR via an unusual mechanism. Plant J. 46 (2), 269–281. https://doi.org/10.1111/j.1365-313X.2006.02690.x.
Jung, S., Ficklin, S.P., Lee, T., Cheng, C.H., Blenda, A., Zheng, P., Yu, J., Bombarely, A., Cho, I., Ru, S., Evans, K., Peace, C., Abbott, A.G., Mueller, L.A., Olmstead, M.A., Main, D., 2014. The Genome Database for Rosaceae (GDR): year 10 update. Nucleic Acids Res. 42, D1237–1244. https://doi.org/10.1093/nar/gkt1012. Database issue.
Kalinka, A.T., Tomancak, P., 2011. Linkcomm: an R package for the generation, visualization, and analysis of link communities in networks of arbitrary size and type. Bioinformatics 27 (14), 2011–2012. https://doi.org/10.1093/bioinformatics/btr311.
Langmead, B., Salzberg, S.L., 2012. Fast gapped-read alignment with Bowtie 2. Nat. Methods 9, 357–359. https://doi.org/10.1038/nmeth.1923.
Lefever, S., Pattyn, F., Hellemans, J., Vandesompele, J., 2013. Single-nucleotide polymorphisms and other mismatches reduce performance of quantitative PCR assays. Clin. Chem. 59 (10), 1470–1480. https://doi.org/10.1373/clinchem.2013.203653.
Legay, S., Guerriero, G., Deleruelle, A., Lateur, M., Evers, D., André, C.M., Hausman, J.-F., 2015. Apple russeting as seen through the RNA-seq lens: strong alterations in the exocarp cell wall. Plant Mol. Biol. 88 (1–2), 21–40. https://doi.org/10.1007/s11103-015-0303-4.
Li, B., Dewey, C.N., 2011. RSEM: accurate transcript quantification from RNA-Seq data with or without a reference genome. BMC Bioinformatics 12 (323), 1–16. https://doi.org/10.1186/1471-2105-12-323.
Love, M.I., Huber, W., Anders, S., 2014. Moderated estimation of fold change and dispersion for RNA-Seq data with DESeq2. Genome Biol. 15. https://doi.org/10.1186/s13059-014-0550-8.
Lu, X., Liu, X., Li, S., Wang, X., Zhang, L., 2011. Possible mechanisms of warming effects for amelioration of superficial scald development on 'Fuji' apples. Postharvest Biol. Technol. 62 (1), 43–49. https://doi.org/10.1016/j.postharvbio.2011.04.008.
Luhua, S., Hegie, A., Suzuki, N., Shulaev, E., Luo, X., Cenariu, D., Ma, V., Kao, S., Lim, J., Gunay, M., Oosumi, T., Lee, S., Harper, J., Cushman, J., Gollery, M., Girke, T., Bailey-Serres, J., Stevenson, R.A., Zhu, J.K., Mittler, R., 2013. Linking genes of unknown function with abiotic stress responses by high-throughput phenotype screening. Physiol. Plant. 148 (3), 322–333. https://doi.org/10.1111/ppl.12013.
Lunn, J., Delorge, I., Figueroa, C., Dijck, P., Stitt, M., 2014. Trehalose metabolism in plants. Plant J. 79 (4), 544–567. https://doi.org/10.1111/tpj.12509.
Luo, F., Yang, Y., Zhong, J., Gao, H., Khan, L., Thompson, D.K., Zhou, J., 2007. Constructing gene co-expression networks and predicting functions of unknown genes by random matrix theory. BMC Bioinformatics 8, 299. https://doi.org/10.1186/1471-2105-8-299.
Lurie, S., Watkins, C.B., 2012. Superficial scald, its etiology and control. Postharvest Biol. Technol. 65, 44–60.
Maniga, A., Ghisaura, S., Perrotta, L., Marche, M., Cella, R., Albani, D., 2017. Distinctive features and differential regulation of the DRTS genes of *Arabidopsis thaliana*. PLoS One 12 (6), 1–35. https://doi.org/10.1371/journal.pone.0179338.
Mattheis, J.P., 2008. How 1-methylcyclopropene has altered the Washington State apple industry. Hortscience 43 (1), 99–101.
Mattheis, J.P., Rudell, D.R., Hanrahan, I., 2017. Impacts of 1-methylcyclopropene and controlled atmosphere established during conditioning on development of bitter pit in 'Honeycrisp' apples. Hortscience 52 (1), 132–137. https://doi.org/10.21273/HORTSCI11368-16.
Oh, Y., Kim, H., Seo, S., Hwang, B., Chang, Y., Lee, J., Lee, D., Sohn, E., Lee, S., Lee, Y., Hwang, I., 2016. Cytochrome b5 reductase 1 triggers serial reactions that lead to iron uptake in plants. Mol. Plant 9 (4), 501–513. https://doi.org/10.1016/j.molp.2015.12.010.
Rehman, H., Nawaz, M., Shah, Z., Ludwig-Müller, J., Chung, G., Ahmad, M., Yang, S., Lee, S., 2018. Comparative genomic and transcriptomic analyses of family-1 UDP glycosyltransferase in three *Brassica* species and *Arabidopsis* indicates stress-responsive regulation. Sci. Rep. 8 (1), 1–18. https://doi.org/10.1038/s41598-018-19535-3.
Rowan, D.D., Hunt, M.B., Fielder, S., Norris, J., Sherburn, M.S., 2001. Conjugated triene oxidation products of alpha-farnesene induce symptoms of superficial scald on stored apples. J. Agric. Food Chem. 49 (6), 2780–2787. https://doi.org/10.1021/jf0015221.
Shannon, P., Markiel, A., Ozier, O., Baliga, N.S., Wang, J.T., Ramage, D., Amin, N., Schwikowski, B., Ideker, T., 2003. Cytoscape: a software environment for integrated models of biomolecular interaction networks. Genome Res. 13 (11), 2498–2504. https://doi.org/10.1101/gr.1239303.
Sisler, E.C., Serek, M., Sisler, E.C., Serek, M., 2003. Compounds interacting with the ethylene receptor in plants. Plant Biol. https://doi.org/10.1055/s-2003-44782.
Soneson, C., Love, M.I., Robinson, M.D., 2015. Differential analyses for RNA-Seq: transcript-level estimates improve gene-level inferences. F1000Research 4, 1–18. https://doi.org/10.12688/f1000research.7563.2.
Thieme, C.J., Rojas-Triana, M., Stecyk, E., Schudoma, C., Zhang, W., Yang, L., Miñambres, M., Walther, D., Schulze, W.X., Paz-Ares, J., Scheible, W.-R., Kragler, F., 2015. Endogenous *Arabidopsis* messenger RNAs transported to distant tissues. Nat. Plants 1 (4). https://doi.org/10.1038/nplants.2015.25.
Tunc-Ozdemir, M., Miller, G., Song, L., Kim, J., Sodek, A., Koussevitzky, S., Misra, A., Mittler, R., Shintani, D., 2009. Thiamin confers enhanced tolerance to oxidative stress in *Arabidopsis*. Plant Physiol. 151 (1), 421–432. https://doi.org/10.1104/pp.109.140046.
Velasco, R., Zharkikh, A., Affourtit, J., Dhingra, A., Cestaro, A., Kalyanaraman, A., Fontana, P., Bhatnagar, S.K., Troggio, M., Pruss, D., Salvi, S., Pindo, M., Baldi, P., Castelletti, S., Cavaiuolo, M., Coppola, G., Costa, F., Cova, V., Ri, A., Goremykin, V., Komjanc, M., Longhi, S., Magnago, P., Malacarne, G., Malnoy, M., Micheletti, D., Moretto, M., Perazzolli, M., Si-Ammour, A., Vezzulli, S., Zini, E., Eldredge, G., Fitzgerald, L.M., Gutin, N., Lanchbury, J., Macalma, T., Mitchell, J.T., Reid, J., Wardell, B., Kodira, C., Chen, Z., Desany, B., Niazi, F., Palmer, M., Koepke, T., Jiwan, D., Schaeffer, S., Krishnan, V., Wu, C., Chu, V.T., King, S.T., Vick, J., Tao, Q., Mraz, A., Stormo, A., Stormo, K., Bogden, R., Ederle, D., Stella, A., Vecchietti, A., Kater, M.M., Masiero, S., Lasserre, P., Lespinasse, Y., Allan, A.C., Bus, V., Chagné, D., Crowhurst, R.N., Gleave, A.P., Lavezzo, E., Fawcett, J.A., Proost, S., Rouzé, P., Sterck, L., Toppo, S., Lazzari, B., Hellens, R.P., Durel, C.-E., Gutin, A., Bumgarner, R.E., Gardiner, S.E., Skolnick, M., Egholm, M., de Peer, Y., Salamini, F., Viola, R., 2010. The genome of the domesticated apple (*Malus* × *domestica* Borkh.). Nat. Genet. 42 (10), 833–839. https://doi.org/10.1038/ng.654.
Wakeel, A., Ali, I., Khan, A., Wu, M., Upreti, S., Liu, D., Liu, B., Gan, Y., 2018. Involvement of histone acetylation and deacetylation in regulating auxin responses and associated phenotypic changes in plants. Plant Cell Rep. 37 (1), 51–59. https://doi.org/10.1007/s00299-017-2205-1.
Watkins, C.B., Bramlage, W.J., Cregoe, B.A., 1995. Superficial scald of 'Granny Smith' apples is expressed as a typical chilling injury. J. Am. Soc. Hortic. Sci. 120 (1), 88–94.
Watkins, C.B., Nock, J.F., Weis, S.A., Jayanty, S., Beaudry, R.M., 2004. Storage temperature, diphenylamine, and pre-storage delay effects on soft scald, soggy breakdown and bitter pit of 'Honeycrisp' apples. Postharvest Biol. Technol. 32 (2), 213–221. https://doi.org/10.1016/j.postharvbio.2003.11.003.
Yang, H.Y., Postel, S., Kemmerling, B., Ludewig, U., 2014. Altered growth and improved resistance of *Arabidopsis* against *Pseudomonas syringae* by overexpression of the basic amino acid transporter AtCAT1. Plant Cell Environ. 37 (6), 1404–1414.
Yoon, G., Kieber, J.J., 2013. 14-3-3 regulates 1-aminocyclopropane-1-carboxylate synthase protein turnover in *Arabidopsis*. Plant Cell 25 (3), 1016–1028. https://doi.org/10.1105/tpc.113.110106.
Yorimitsu, T., Sato, K., Takeuchi, M., 2014. Molecular mechanisms of Sar/Arf GTPases in vesicular trafficking in yeast and plants. Front. Plant Sci. 5, 1–12. https://doi.org/10.3389/fpls.2014.00411.
Zermiani, M., Zonin, E., Nonis, A., Begheldo, M., Ceccato, L., Vezzaro, A., Baldan, B., Trentin, A., Masi, A., Pegoraro, M., Fadanelli, L., Teale, W., Palme, K., Quintieri, L., Ruperti, B., 2015. Ethylene negatively regulates transcript abundance of ROP-GAP rheostat-encoding genes and affects apoplastic reactive oxygen species homeostasis in epicarps of cold stored apple fruits. J. Exp. Bot. 66 (22), 7255–7270. https://doi.org/

10.1093/jxb/erv422.
Zhang, X.F., Jiang, T., Wu, Z., Du, S.Y., Yu, Y.T., Jiang, S.C., Lu, K., Feng, X.J., Wang, X.F., Zhang, D.P., 2013. Cochaperonin CPN20 negatively regulates abscisic acid signaling in *Arabidopsis*. Plant Mol. Biol. 83 (3), 205–218.
Zhao, S., Guo, Y., Sheng, Q., Shyr, Y., 2014. Advanced heat map and clustering analysis using Heatmap3. Biomed Res. Int. 1–6. https://doi.org/10.1155/2014/986048.
Zhao, Y., Chan, Z., Gao, J., Xing, L., Cao, M., Yu, C., Hu, Y., You, J., Shi, H., Zhu, Y., Gong, Y., Mu, Z., Wang, H., Deng, X., Wang, P., Bressan, R.A., Zhu, J.-K., 2016. ABA receptor PYL9 promotes drought resistance and leaf senescence. Proc. Natl. Acad. Sci. 113 (7), 1949–1954. https://doi.org/10.1073/pnas.1522840113.
Zheng, Y., Liao, C., Zhao, S., Wang, C., Guo, Y., 2016. The glycosyltransferase QUA1 regulates chloroplast-associated calcium signaling during salt and drought stress in *Arabidopsis*. Plant Cell Physiol. https://doi.org/10.1093/pcp/pcw192.